JOURNAL OF AIRCRAFT
Vol. 40, No. 2, March–April 2003

Wind-Tunnel Study on a 65-deg Delta Wing at Sideslip

N. G. Verhaagen*
Delft University of Technology, 2600 GB Delft, The Netherlands
and
C. E. Jobe†
U.S. Air Force Research Laboratory, Dayton, Ohio 45433

The leeward vortices occurring over low-aspect-ratio delta wings typical of many current fighter aircraft cause highly nonlinear forces and moments. Near stall the vortices break down over the wing surface and introduce additional discontinuities and transients in the aerodynamics. Experimental studies of these flows are needed to develop mathematical models to represent the interaction between the vehicle motion and the forces and moments. The models will permit design for increased maneuverability in future fighters. Many static and dynamic tests of a common 65-deg swept delta wing in pitch and roll were conducted. Here, the effects of sideslip on the flow over a flat-plate 65-deg swept delta wing tested at a geometric angle of attack of 30 deg are described. At this angle of attack, the major part of the flow over the wing is affected by vortex core breakdown. Sideslip causes a strong asymmetry in the breakdown location. This is shown to have a large effect on the surface flow and pressures and on the normal force and pitching moment.

Nomenclature

b	=	wing span
C_L	=	lift coefficient
C_m	=	pitching-moment coefficient
C_N	=	normal-force coefficient
C_n	=	yawing-moment coefficient
C_p	=	static-pressure coefficient
C_T	=	tangential-force coefficient
C_Y	=	lateral-force coefficient
c	=	root chord length
s	=	local wing semispan
t	=	wing thickness
x, y, z	=	coordinates of wing-axes system
α, AoA	=	angle of attack
β, AoS	=	angle of sideslip
ϕ	=	angle of roll

Introduction

MODERN fighter aircraft are designed to rely on the lift generated by vortex flow to enhance maneuverability. Strong vortices generated at the leading edge of highly swept lifting surfaces are part of the overall flowfield of such aircraft and can have a dominant effect on the flow and the air loads. At high angles of attack, a sudden change in the vortex flowfield occurs when the core of the vortex breaks down over the wing surface. This change in flow structure causes strong nonlinearities in the aircraft's aerodynamic behavior. Studies by Huang et al.[1] and Jenkins[2] indicate that the aerodynamics at these conditions depends on both time and motion history.

Studies of the flow phenomena occurring at near- and post-stall conditions are essential to meet the requirement of increasing maneuverability of current and future fighters. At the Air Vehicles Directorate of the U.S. Air Force Research Laboratory (AFRL) and the Institute for Aerospace Research (IAR) of the National Research Council of Canada, studies are being conducted to help develop mathematical models that simulate the aerodynamic nonlinearities encountered during dynamic flight conditions. Static and dynamic tests were conducted on a common 65-deg swept delta wing. The model, shown in Fig. 1, has sharp leading and trailing edges that are symmetrically beveled at an angle of 20 deg. Most data were taken with a rolling model at a Mach number of 0.3 and a chord Reynolds number of 3.6 million. The rolling model was tested on a sting at an angle of 30 deg. The static tests indicate the existence of critical states at specific angles of roll (Fig. 2). A critical state is characterized by a discontinuity in the static force-and-moment curves. The critical states are important to flight mechanics as finite time is required for the transition from one flow state to the other. The test data confirm the existence of strong nonlinearities in the forces and moments and a dependency on the motion history. Based on a nonlinear-indicial-response model, Grismer and Jenkins[3] have developed a theory that simulates the nonlinear aerodynamic behavior near the critical states.

Huang et al.[1] conducted extensive flow-visualization tests to study the changes in the flow topology under static conditions associated with the critical states. Several characteristic surface patterns were identified, and, based on these patterns, possible corresponding three-dimensional flowfield topologies were inferred. Interpretation of the surface patterns was complicated because of the beveling of the model and the presence of a tangent-ogive centerbody. To avoid these complications, within the framework of an EOARD contract, a study has been conducted using two models of a simple flat-plate 65-deg delta wing. The models were constructed from Duralumin plate and tested in a low-speed wind tunnel at the Delft University of Technology (TUD) in the Netherlands. The wings were tested at a fixed (geometric) α of 30 deg and at angles of sideslip up to 20 deg. Huang et al.[1] carried out their tests on a rolling model. This was not possible in the TUD tunnel because the model support system does not permit the model to rotate about its roll axis. The data of Fig. 2, however, show that there is a correlation between the roll critical states and the sideslip critical states. Flow-visualization tests, surface-pressure and balance measurements were performed and have been reported in papers by Verhaagen[4] and Verhaagen and Jobe.[5]

The present paper describes the experiment, corrections and results of the tests conducted on the 65-deg delta wings.

Experimental Setup and Conditions

The geometry of the flat-plate delta wings is given in Fig. 3. The wings have a chord length of 0.665 m and a semispan of 0.620 m.

Received 16 March 2001; revision received 12 November 2002; accepted for publication 12 November 2002.

*Research Scientist, Faculty of Aerospace Engineering, P.O. Box 5058. Senior Member AIAA.
†Aerospace Engineer. Associate Fellow AIAA.

Their thickness is 20 mm; the leading and trailing edges are sharp and beveled on only the lower (windward) surface at 31 and 23 deg, respectively. The wings were tested in the Low-Turbulence-Tunnel of the Department of Aerospace Engineering of TUD. This is a closed-circuit tunnel with an octagonal test section 1.80 m wide, 1.25 m high, and 2.60 m long. The tests were conducted at an airspeed of 50 m/s, yielding a chord Reynolds number of 2.3×10^6. Each wing was suspended at the $x = 0.515$ m ($x/c = 0.775$) position through a streamlined strut that is connected to the balance system overhead of the test section (Fig. 4). The wings were tested at a geometric α of 30 deg and at β up to 20 deg. To avoid interference of the strut with the vortex flow, the wings were tested inverted, that is, with their flat leeward surface facing down. In literature, it is common to present data of delta wings with their leeward surface facing up. This surface is then called the "upper" surface. This terminology will also be used in the present paper.

One wing was used for balance measurements and flow-visualization tests, the other one, provided with pressure taps, was used to take surface pressures. On the upper surface of the latter wing, the taps are located on 15 spanwise rows, from $x/c = 0.10$ to 0.99. The longest rows near the trailing edge contained a maximum of 33 taps. On the lower surface there are taps at $x/c = 0.30$, 0.50, and 0.70, with a maximum of 19 taps per row. The distribution of the taps is identical on the left and right half of the wing. Each tap has a diameter of 0.20 mm. The pressures were recorded using an automatic multimanometer with an accuracy of 1 Pa.

Flow-visualization tests were conducted to study the effect of β on the flow on and off the wing. The high airspeed and large angle of attack generated very low pressures and temperatures in the cores of the leading-edge vortices. Consequently, as shown in Fig. 4, natural condensation could be seen to occur in the cores. Still photographs and analog video recordings were taken to study the effect of β on the vortex-core trajectory and breakdown point.

The flow pattern on the lower and upper surface of the wing was visualized using two mixtures. One mixture, briefly called oil-flow mixture, consisted of a mixture of titanium dioxide, pipe clay, a surface tension relaxator, and kerosene. The other was a mixture of fluorescent dye and oil. To visualize the latter, the wing was illuminated using ultraviolet light. Figure 5a shows the upper-surface pattern for $\beta = 10$ deg visualized with the oil-flow mixture, whereas Fig. 5b gives the pattern for $\beta = 5$ deg visualized with the other mixture. Compared to the oil-flow mixture, the fluorescent-dye mixture has the advantage that it does not dry while the tunnel is running, making it possible to observe the changes to the surface pattern with running time, or to a changing β. The mixture very well resolved the location of the secondary-separation lines, but outside these lines the resolution was poor compared to that of the pattern visualized with

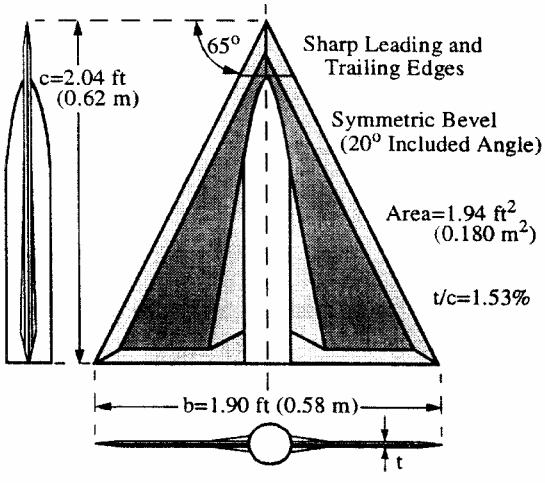

Fig. 1 AFRL/IAR-wing.

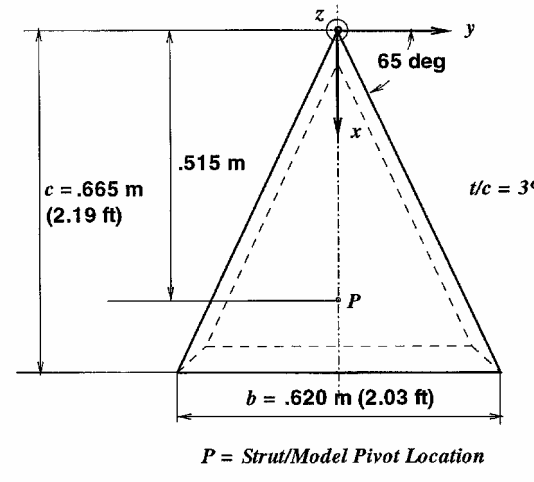

Fig. 3 TUD-wing geometry.

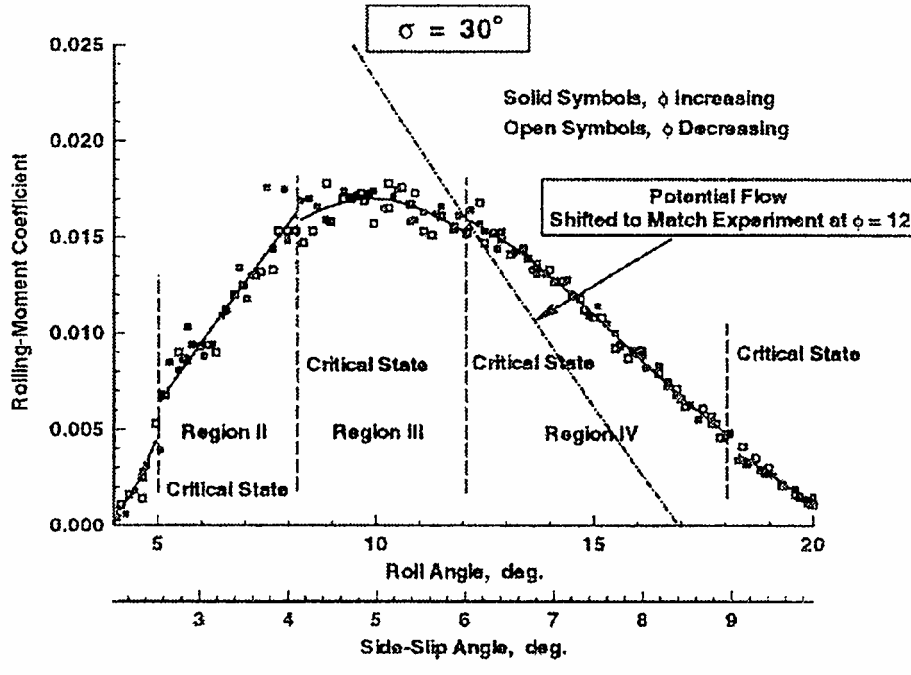

Fig. 2 Effect of ϕ and β on rolling-moment coefficient (Jenkins[2]).

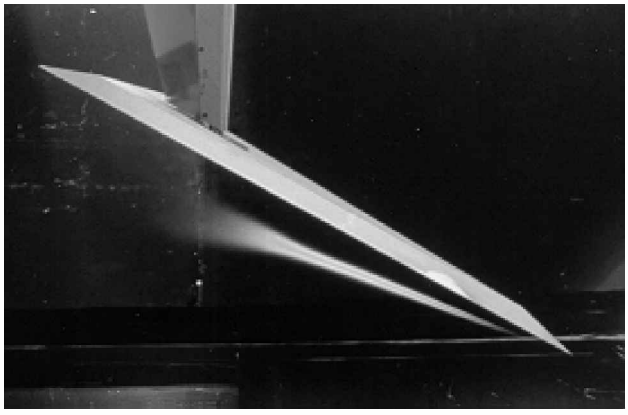

Fig. 4 Condensation of vortex cores.

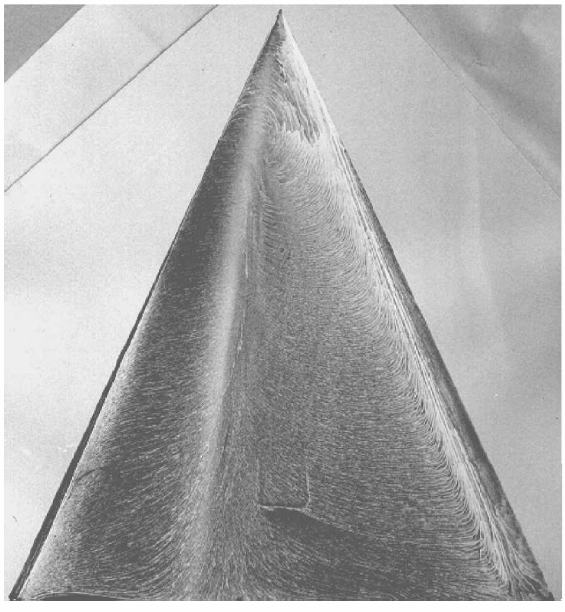

a) Oil flow

b) Fluorescent-dye/oil

Fig. 5 Upper-surface flow pattern visualized using different mixtures.

the oil-flow mixture. Still photographs and digital video recordings were taken of the patterns visualized with both mixtures.

Static time-averaged force-and-moment data were obtained using a six-component balance system. The data were taken at β increasing from -20 to $+20$ deg and decreasing again to -20 deg. Three data sets were generated by taking data at β steps of 1.0, 0.5, and 0.1 deg, respectively. The data were corrected for the elastic deformation of the strut and the balance system under aerodynamic load and for strut/model interference effects. The force coefficients are based on freestream dynamic pressure and wing area. The moment coefficients are, in addition, based on chord (C_m) or span (C_l and C_n) as reference length. The moments are given in the wing-axes system, relative to the strut/model pivot location at $x/c = 0.775$.

As far as tunnel-wall-interference corrections are concerned, existing theories estimate corrections that can be applied for delta wings only if α is less than 25 deg, β is zero, and if vortex breakdown does not take place over the wing.[6] The best way to obtain an idea of the order of magnitude of the wall corrections at zero β is to use the theory developed by Hsing and Lan.[7] Based on this theory, at the present test conditions the blockage is estimated to be of the order of 7%, whereas the upflow angle is estimated to be as large as 5 deg. The blockage correction has been applied to the dynamic pressure used to nondimensionalize balance and pressure data.

Although α was 30 deg at zero airspeed, the elastic deformation of the strut and balance system under aerodynamic load and the tunnel-wall-interference effects are estimated to yield an effective α as large as 36 deg! In the next section it will be shown that at zero β vortex breakdown occurs at $x/c = 0.20$. Based on Fig. 4 of Jobe,[8] the α correction of 6 deg correlates the vortex breakdown location with data of other experiments on 65-deg delta wings.

Test Results

Off-Surface Flow Visualization

At zero β breakdown occurs at $x/c = 0.20$. The breakdown location was defined to coincide with the point of sudden expansion of the core into diffuse turbulence. The effect of β (or AoS) on the location of the breakdown point is shown in Fig. 6. The breakdown point on the leeward wing half moves into the downstream direction with increasing β, whereas on the windward half this point moves towards the apex. This correlates with the observation that an increase of the leading-edge sweep of a delta wing tends to increase the distance from the breakdown point to the apex.[9,10] The breakdown point was observed to be symmetric with respect to β up to 8 deg. Above this angle the cores could not be observed. Video recordings were used to estimate the amplitude and frequency of the oscillation of the breakdown point along the core axis. Error bars in Fig. 6 mark the estimated range of the breakdown points at each β. The

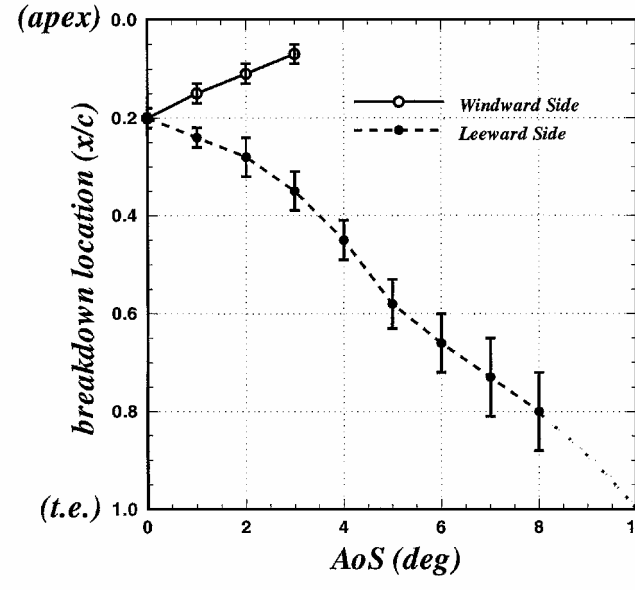

Fig. 6 Effect of β on breakdown point.

amplitude of the oscillations increased from 3% chord at zero β to about 18% chord at $\beta = 8$ deg. The points were observed to oscillate at a frequency of 4–5 Hz. Beyond $\beta = 5$ deg the condensation along the entire core became interrupted with about the same frequency. The intermittent condensation of the core might be caused by instability in the formation of the vortex near the apex. Associated with this stream-wise instability are strong pressure fluctuations in the vortex flow. This resulted in a loud flapping noise that was audible in the tunnel at β between 6 and 12 deg. The cause of this instability is not clear and needs further investigation.

Surface Flow Visualization

Based on the still and video recordings of the surface flows, in Figs. 7 and 8 schematics are given of the streamline patterns observed on the lower and upper surface. Schematics are preferred over prints of the photographs or video frames because from prints it is not always easy to distinguish surface flow details. To show the pattern of both surfaces at similar β, the pattern on the lower surface is presented such as one would see from the inside of the model, if the model were made of a transparent material. Short-dashed lines mark the inboard boundary of the beveled edges on this surface. The transition from the beveled edges to the flat lower surface is sharp, not rounded. For reference, the inside corners of the transition lines are marked A, B, and C. On both the lower and upper surface a long dash-dot line is used to mark the centerline of the wing. Solid lines (or curves) are used to indicate surface streamline or skin-friction lines, as well as separation and attachment lines.

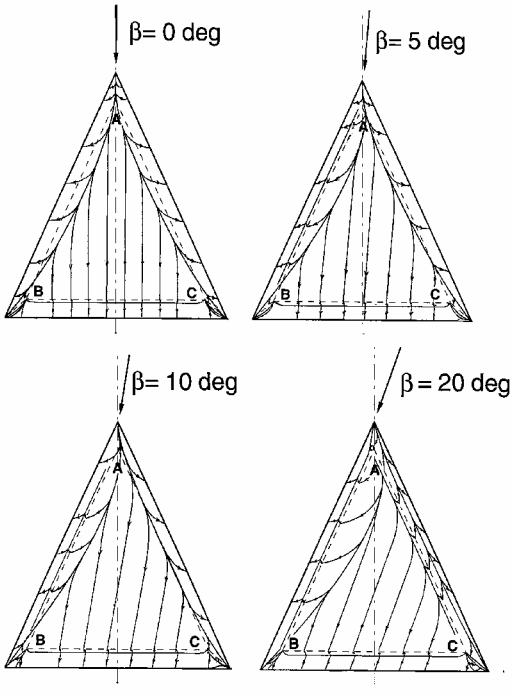

Fig. 7 Effect of β on lower-surface pattern.

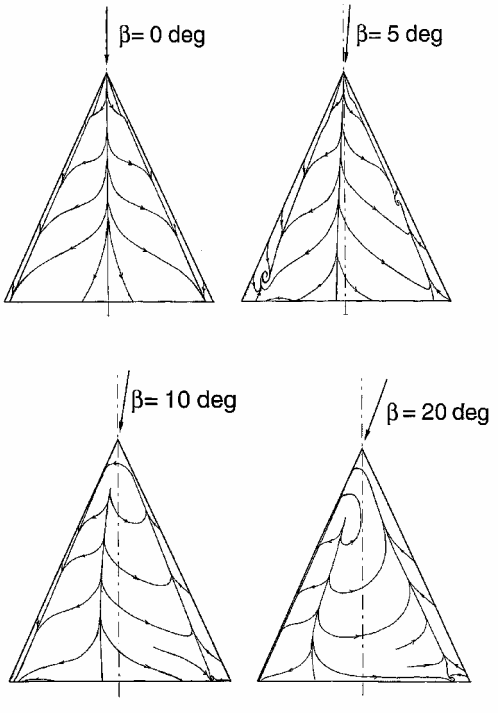

Fig. 8 Effect of β on upper-surface pattern.

First, the effect of β on the streamline pattern on the lower surface, illustrated in Fig. 7, is described. At zero β an attachment line is visible at the centerline of the beveled nose. A stagnation point can be presumed to be present on this line. The resolution of the flow pattern, however, was not sufficient to resolve the location of this point. Downstream of the nose, the attachment line splits into two separate lines. Outboard of these lines, the shear flow bends towards the leading edge. The shear layer leaves the wing at this edge to mix with the shear layer from the upper surface into a free shear layer that rolls up into a primary vortex. Inboard of the two attachment lines on the lower flat surface, the skin-friction lines are parallel to the wing centerline and directed towards the trailing edge. Downstream of bevel line BC the flow pattern gives evidence of a bubble type of boundary-layer separation. An attachment line is visible between this line and the trailing edge.

If the wing is put into sideslip, the general trend is that the attachment lines displace into the windward direction. From $\beta = 5$ deg a bubble type of separation of the outward directed boundary layer becomes visible outboard of bevel line AB. From $\beta = 10$ deg a similar type of separation is visible inboard of bevel line AC. This separation is caused by the sharp transition between the beveled edges and the central surface and might not occur on wings that have a smoother transition between these surfaces. At the nose and wing tips, complex changes in the streamline pattern occur with β. These are discussed in detail in Ref. 5.

Figure 8 shows the effect of β on the upper-surface flow. At zero β an attachment line is visible along the centerline of the wing. Near the leading edge a secondary-separation line can be discerned with a kink at $x/c \approx 0.16$, marking the transition region of the boundary layer on the upper surface. Upstream of this region a tertiary-separation line was visible between the leading edge and the secondary-separation line (this line has not been drawn in Fig. 8). If the wing is yawed to a positive β, the attachment line moves off center towards the leeward leading edge. The kink in the secondary-separation line, which marks the boundary-layer transition region, moves upstream on the windward half and into the opposite direction on the other half. From $\beta = 4$ deg a whorl adjoining the secondary-separation line is visible near the leeward tip. The direction of rotation of this whorl is in the clockwise direction. Earnshaw and Lawford[11] (E. & L.) found similar whorls on the surface of their series of sharp-edged delta wings tested at zero β, for example, on the tips of a 76-deg delta wing at $\alpha = 35$ deg. This α is close to the present one, and at $\beta = 5$ deg the effective sweep of the leeward leading edge of the present delta wing is 70 deg. E. & L. suggest that the whorl is as a result of an off-surface separation of the secondary vortex, but to the authors' knowledge there exists no experimental evidence of this type of separation. Flowfield surveys could help verify its existence. E. & L. further observed that the whorl moved towards the apex with increasing α. The present tests indicate that this is not the case if sideslip is involved; the whorl is not displaced much when β increases from 4 to 8 deg and disappears at larger β. A similar type of whorl, but with a counterclockwise sense of rotation, is visible at the windward wing tip from $\beta = 3$ deg. The whorl moves rapidly upstream with increasing β and is at $x/c = 0.60$ when $\beta = 5$ deg. Downstream of this whorl a reversal of the skin-friction lines is visible. This reversal is thought to be caused by a bluff-body type of wake flow downstream of the breakdown location.

Upstream of the whorl a vortex-induced type of streamline pattern remains.

At $\beta = 10$ deg a vortex-induced streamline pattern is evident on the leeward half, whereas on the other half most of the skin-friction lines are reversed. On the front part of the wing, a region of circulating weak shear flow is observed.

From $\beta = 10$ to 20 deg, the variations in the surface flow pattern are small. Compared to $\beta = 10$ deg, at 20 deg the region of circulating flow is located more downstream and closer to the leeward edge. Associated with this is a shift of the attachment line into the leeward direction. From $\beta = 10$ deg a counterclockwise rotating whorl is visible near the trailing edge on the windward half. Beyond $\beta = 16$ deg the distance between the secondary-separation line and the leeward leading edge becomes very small. It is believed that a secondary vortex is no longer formed at larger β. Between the separation line and the attachment line, a vortex-induced streamline pattern remains visible. The pattern that is formed by the skin-friction lines can be considered as a continuous vector field in which critical (or singular) points occur where the skin friction is zero. Jobe et al.[12] discuss the topology of flow over delta wings and give a survey of literature on this subject. The effect of β on the topology of the flow over the present delta wing will be discussed in a follow-up paper. With the streamline patterns just described it is possible to determine the topology of the flow on both surfaces of the wing and at the trailing edge. The only region still lacking detailed information is the apex.

The flow patterns help to obtain an idea of the effect of β on the flow off the upper surface of the delta wing. Up to $\beta = 8$ deg, the flow over the wing can be expected to be dominated by two primary and secondary vortices. Near the apex tertiary vortices are generated. The vortices shift towards the leeward edge with increasing β. The leeward secondary vortex is believed to reduce in size and has vanished when β is larger than 16 deg. Beyond $\beta = 9$ deg the flow over the windward half of the wing is thought to be dominated by a large turbulent bubble type of flow that is thought to originate from a region of circulation on the front part of the wing. More evidence on the effect of β on the location and structure of the vortices could be obtained from surveys of the vorticity and pressure distribution of the flow off of the delta wing.

Surface-Pressure Measurements

The effects of β on the measured surface-pressure distribution are described in detail in Ref. 4. Only the major effects will be discussed here. Figure 9 shows the effects on the upper-surface negative C_p. Repeatability tests indicate an uncertainty in C_p of ± 0.01. At β (or AoS) $= 0$ deg the magnitude of negative C_p or suction induced by vortices is strong up to $x/c = 0.20$, whereas downstream of this station the suction peaks decrease in level and extend in the lateral direction. The latter is because the vortex core becomes turbulent and extends in the radial direction downstream of the breakdown point. Such an effect of vortex breakdown on the shape of the C_p curves has also been observed in other experiments.[13,14] When the delta wing is yawed to $\beta = 10$ deg, the displacement of the vortices shifts the suction peaks into the leeward direction. On the leeward wing half, a strong reduction of the suction can be noted on the front part of the wing, whereas a slight increase is visible on the rear part. The latter can be associated with the downstream displacement of the breakdown point on this wing half. On the windward half the breakdown point moves upstream, resulting in a reduction of the suction, especially at the most forward stations. On the rear part, the suction reduces towards the trailing edge. The value of the integrated upper-surface C_p, or suction force, is the largest on the windward half. When β is increased further to 20 deg, a reduction of the suction and flattening of the curves continues to occur on the front part of the wing. The upper-surface streamline pattern gave evidence of a region of circulating weak shear flow on this part of the wing. This might have caused the strong reduction of the suction here. Further downstream, low suction peaks remain visible on the leeward half of the wing. The surface streamline pattern suggests that a primary vortex is still active there. The low suction might be caused by low vortex strength and/or a distant location of the vortex from the wing. The suction force on the leeward wing half is much lower than that on the opposite half.

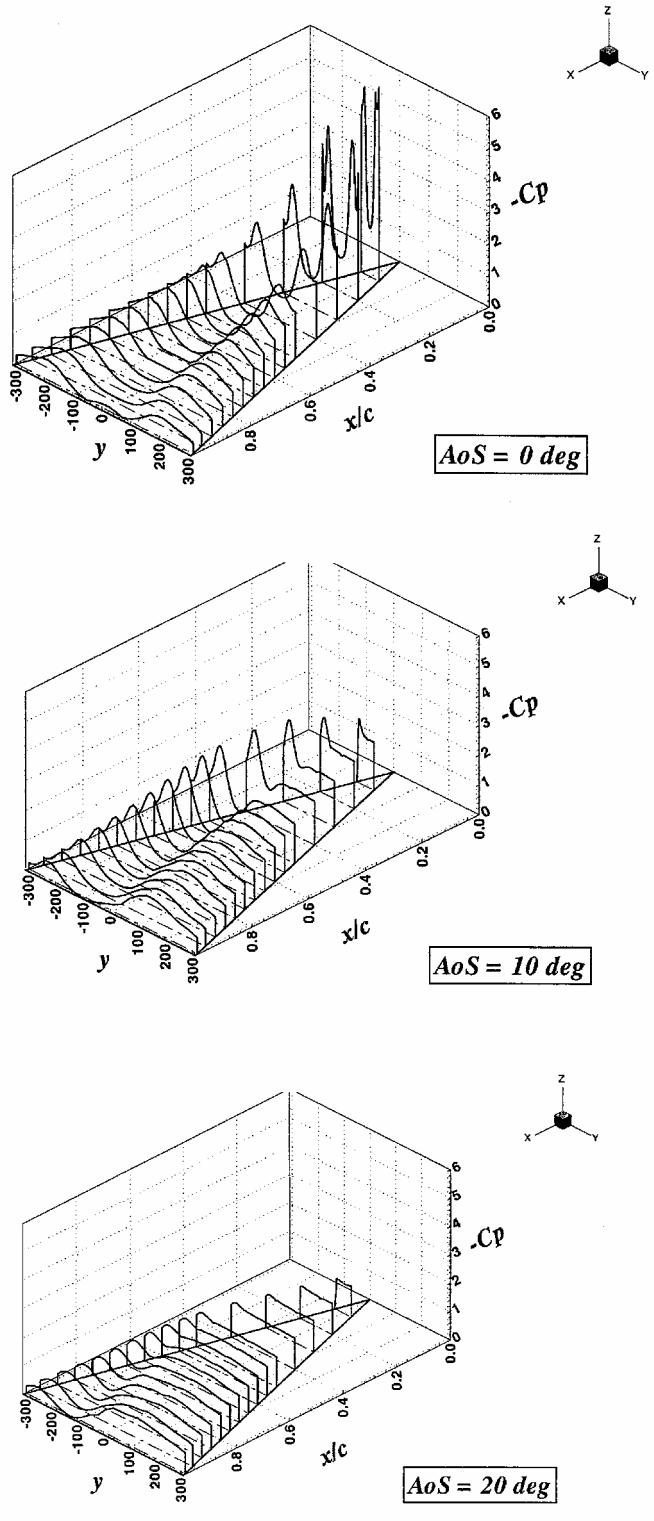

Fig. 9 Effect of β on upper-surface pressure distribution.

Figure 10 shows the effect of β on the lower- and upper-surface C_p at $x/c = 0.50$. As just described, the C_p on the upper surface is strongly affected by β. The effect on the C_p on the lower surface is smaller. With increasing β the C_p on this surface can be seen to decrease if y/s is smaller and to increase if y/s is larger than +0.50. The latter tendency was also evident in the C_p data recorded at $x/c = 0.30$ and 0.70. The C_p distribution suggests that the stagnation point moves towards the windward leading edge with increasing β. This correlates with the displacement of the attachment line noted in Fig. 7.

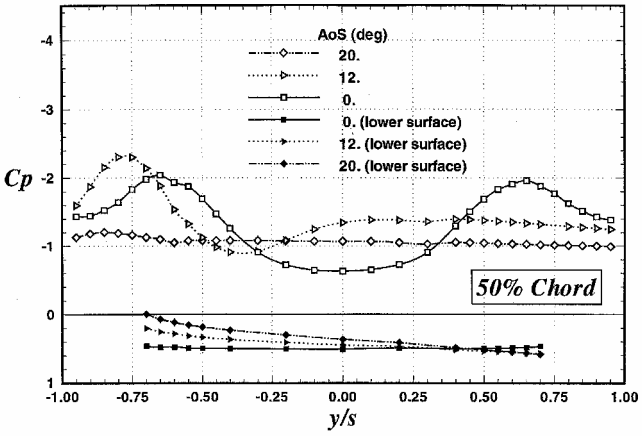

Fig. 10 Effect of β on C_p distribution at $x/c = 0.50$.

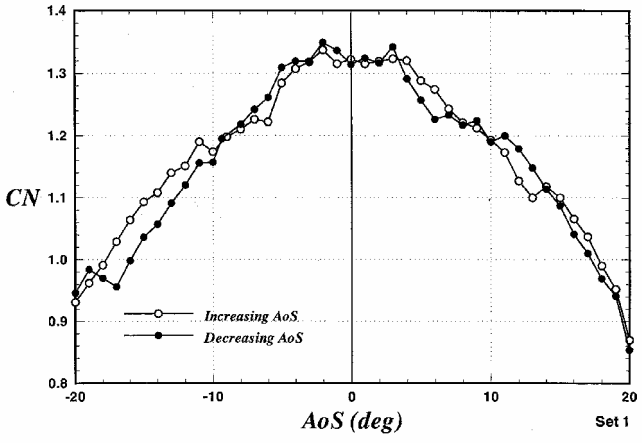

Normal-force coefficient

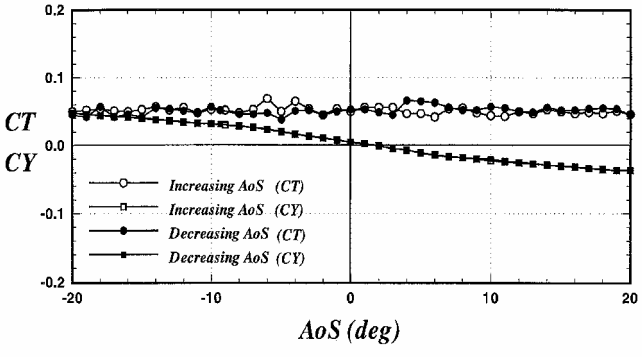

Tangential and lateral-force coefficient

Fig. 11 Effect of β on force coefficients.

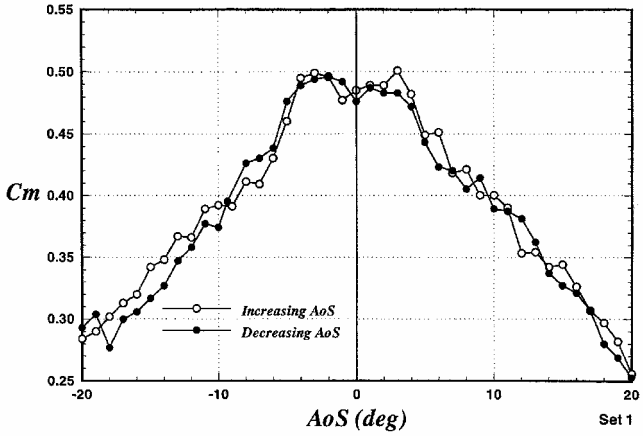

Pitching-moment coefficient

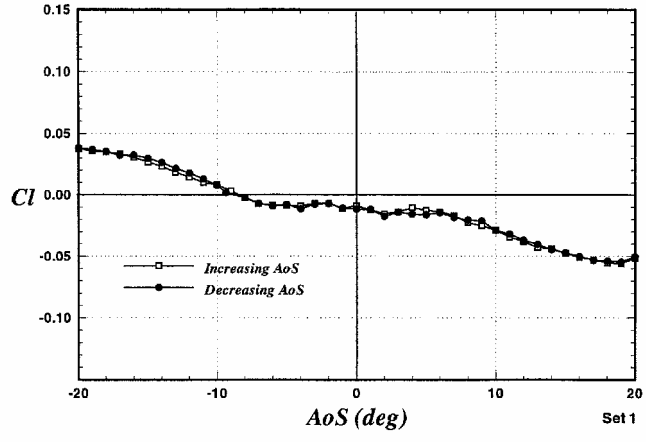

Rolling-moment coefficient

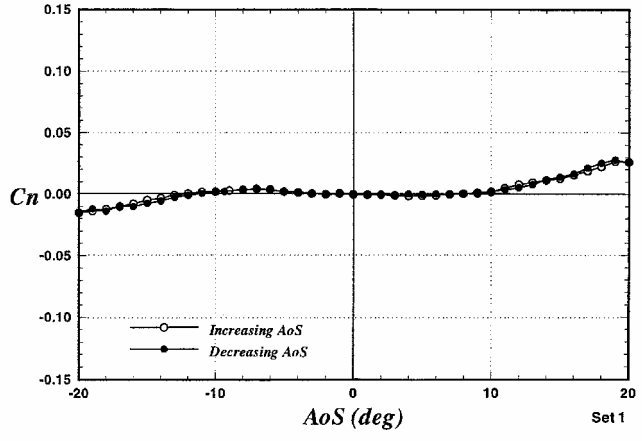

Yawing-moment coefficient

Fig. 12 Effect of β on moment coefficients.

Forces and Moments

Figure 11 shows a plot of the force data. Only the data taken at β between -20 and $+20$ deg, in steps of 1.0 deg, are shown here. The difference between the runs with increasing β (open symbols) and decreasing β (solid symbols) gives an indication of hysteresis of the data. Sideslip has a large effect on C_N. The slight increase of this coefficient when β increases from 0 to 3 deg might be caused by the increase of the suction on the leeward half of the upper surface. At larger β, C_N reduces considerably because of the decreasing suction on the wing upper surface. Nonlinearity and hysteresis loops are visible in the C_N curves. As far as the other force coefficients are concerned, the plots indicate that β has little effect on C_T and only a small effect on C_Y.

The effect of β on moment coefficients is illustrated in Fig. 12. The effect on the pitching-moment coefficient C_m is similar to that on C_N. A strong reduction is measured when β is larger than 3 deg because of the reduction of the suction on the front part of the upper surface. The effect on C_l and C_n is smaller. The C_l curves have a negative gradient at large β. This is because of the decreasing suction force on the leeward half of the upper surface. C_l should, theoretically, be equal to zero at $\beta = 0$ deg. That this is not the case in the present experiment might be because of a small asymmetry in the geometry of the model. No special tests were carried out to check the repeatability of the balance data. As far as the largest coefficients are concerned, comparison of the data taken at identical (α, β) combinations indicates a maximum uncertainty in C_N and C_m of ± 0.030 and ± 0.010, respectively.

Conclusions

Wind-tunnel tests were conducted to generate data on the effect of β on the flow over a flat-plate 65-deg delta wing at high α.

Although α was exactly 30 deg at zero airspeed, the elastic deformation of the strut and balance system and the tunnel-wall-interference effects are estimated to yield an effective α as large as 36 deg.

Vortex breakdown has a dominant effect on the flow over the delta wing. At zero β vortex breakdown occurs already at 20% chord. With sideslip the breakdown location moves towards the apex on the windward wing half and into the opposite direction on the leeward wing half. The amplitude of the oscillation of the breakdown point along the vortex axis tends to increase with β.

The effect of β on the surface streamline pattern is complex. Most changes in the pattern are observed to occur in the range $|\beta| < 10$ deg. Schematics showing details of the streamline pattern on both surfaces of the wing help to determine the effect of β on the topology of the surface flow. Based on the streamline patterns, suggestions are made for the changes because of β of the structure of the flow above the wing. To confirm these suggestions, detailed surveys of the flowfield over the delta wing are recommended.

It is also observed that sideslip has a large effect on the normal force and, associated with this, the pitching moment. The effect on the other forces and moments is smaller and of the same order of magnitude. Hysteresis effects are apparent in the force-and-moment curves. Discontinuities in the curves might be indicative of the presence of critical states. These critical states will be analyzed in a subsequent paper.

Acknowledgments

The authors would like to thank Bertus Keus and Leo Molenwijk for their assistance during the tests in the Low-Turbulence-Tunnel. This study was supported by the Air Force Office of Scientific Research under EOARD Contract SPC 97-4067 with Charbel Raffoul as monitor.

References

[1]Huang, X. Z., Hanff, E. S., and Jobe, C. E., "Surface Flow Topology on a Delta Wing at High Incidence for a Range of Roll Angles," AIAA Paper 96-2398, June 1996.

[2]Jenkins, J. E., "Nonlinear Aerodynamic Characteristics of a 65 Degree Delta Wing in Rolling Motion: Implications to Testing and Flight Mechanics Analysis," AIAA Paper 97-0742, Jan. 1997.

[3]Grismer, D. S., and Jenkins, J. E., "Critical-State Transients for a Rolling 65-deg Delta Wing," *Journal of Aircraft*, Vol. 34, No. 3, 1997, pp. 380–386.

[4]Verhaagen, N. G., "Effect of Sideslip on the Flow over a 65-deg Delta Wing," AIAA Paper 2000-0977, Jan. 2000.

[5]Verhaagen, N. G., and Jobe, C. E., "Study on a 65-deg Delta Wing at Sideslip," AIAA Paper 2001-0691, Jan. 2001.

[6]Verhaagen, N. G., "Tunnel Wall Effect on the Flow Around a 76/40-deg Double-Delta Wing," AIAA Paper 98-0312, Jan. 1998.

[7]Hsing, C.-C. A., and Lan, C. E., "Low-Speed Wall Interference Assessment/Correction with Vortex Flow Effect," *Journal of Aircraft*, Vol. 34, No. 2, 1997, pp. 220–227.

[8]Jobe, C. E., "Vortex Breakdown Location over 65-deg Delta Wings; Empiricism and Experiment," AIAA Paper 98-2526, June 1998.

[9]Huang, X. Z., Sun, Y. Z., and Hanff, E. S., "Further Investigations of Leading-Edge Vortex Breakdown over Delta Wings," AIAA Paper 97-2263, June 1997.

[10]Wentz, W. H., and Kohlman, D. L., "Vortex Breakdown on Slender Sharp-Edged Wings," *Journal of Aircraft*, Vol. 8, No. 3, 1997, pp. 156–161.

[11]Earnshaw, P. B., and Lawford, J. A., "Low-Speed Wind-Tunnel Experiments on a Series of Sharp-Edged Delta Wings," Aeronautical Research Council, R. & M. 3424, London, May 1966.

[12]Jobe, C. E., Hsia, A. H., Jenkins, J. E., and Addington, G. A., "Critical States and Flow Structure on a 65-Deg Delta Wing," *Journal of Aircraft*, Vol. 33, No. 2, 1996, pp. 347–352; also AIAA Paper 94-3479, Aug. 1994.

[13]Verhaagen, N. G., and Naarding, S. H. J., "Experimental and Numerical Investigation of the Vortex Flow over a Sideslipping Delta Wing," *Journal of Aircraft*, Vol. 26, No. 11, 1989, pp. 971–978.

[14]Papadakis, M., Phillis, D., and Liu, X., "Experimental and Numerical Delta Wing Study at High Angles of Attack and Sideslip," AIAA Paper 92-2713, June 1992.